



**Queensland University of Technology**  
Brisbane Australia

This is the author's version of a work that was submitted/accepted for publication in the following source:

Frost, Ray L., Xi, Yunfei, Pogson, Ross E., Millar, Graeme J., Tan, Keqin, & Palmer, Sara J. (2012) Raman spectroscopy of synthetic CaHPO<sub>4</sub>•2H<sub>2</sub>O—and in comparison with the cave mineral brushite. *Journal of Raman Spectroscopy*, 43(4), pp. 571-576.

This file was downloaded from: <http://eprints.qut.edu.au/49789/>

**© Copyright © 2011 John Wiley & Sons, Ltd.**

**Notice:** Changes introduced as a result of publishing processes such as copy-editing and formatting may not be reflected in this document. For a definitive version of this work, please refer to the published source:

<http://dx.doi.org/10.1002/jrs.3063>

# Raman spectroscopy of synthetic CaHPO<sub>4</sub>·2H<sub>2</sub>O – and in comparison with the Cave mineral brushite

3 Ray L. Frost,<sup>1</sup> • Yunfei Xi,<sup>1</sup> Ross E Pogson,<sup>2</sup> Graeme J. Millar,<sup>1</sup> Keqin Tan<sup>1</sup> and  
4 Sara J Palmer<sup>1</sup>

<sup>5</sup> Chemistry Discipline, Faculty of Science and Technology, Queensland University of  
<sup>6</sup> Technology, GPO Box 2434, Brisbane Queensland 4001, Australia.

<sup>8</sup> <sup>2</sup>Mineralogy & Petrology, Australian Museum, 6 College St., Sydney, NSW, Australia 2010

9 Abstract

10 The mineral brushite has been synthesised by mixing calcium ions and hydrogen phosphate  
11 anions to mimic the reactions in a Cave. The vibrational spectra of the synthesised brushite  
12 were compared with that of the natural Cave mineral. Bands attributable to the  $\text{PO}_4^{3-}$  and  
13  $\text{HPO}_4^{2-}$  anions are observed. Brushite, both synthetic and natural, is characterised by an  
14 intense sharp band at  $985 \text{ cm}^{-1}$  with a shoulder at  $1000 \text{ cm}^{-1}$ . Characteristic bending modes  
15 are observed in the  $300$  to  $600 \text{ cm}^{-1}$  region. The spectra of the synthesised brushite matches  
16 very well the spectrum of brushite from the Moorba Cave, Western Australia.

17

**18 Key words:** brushite, monetite, phosphate, Raman spectroscopy, infrared spectroscopy

19

\* Author to whom correspondence should be addressed (r.frost@qut.edu.au)

20    **Introduction**

21    Brushite is a mineral with the chemical formula  $\text{CaHPO}_4 \cdot 2\text{H}_2\text{O}$ . The mineral is understood to  
22    be a precursor of apatite and is found in guano-rich Caves, formed by the interaction of guano  
23    with calcite at a low pH <sup>1,2</sup>. It forms crystals of prismatic shape having a monoclinic crystal  
24    structure. The mineral will transform to monetite upon dehydration. Brushite is found in  
25    kidney stones <sup>3-7</sup>. However the mineral is often found in Caves and is often regarded as a  
26    ‘Cave’ mineral <sup>8,9</sup>. The mineral has been identified in quite a large number of Australian  
27    Caves including the Skipton lava tube Caves (southwest of Ballarat, Victoria, Australia) and  
28    at Moorba Cave (Jurien Bay, Western Australia). As such, many minerals formed in these  
29    Caves besides brushite include archerite  $(\text{K},\text{NH}_4)(\text{H}_2\text{PO}_4)$  <sup>10</sup>, mundrabillaite  
30     $(\text{NH}_4)_2\text{Ca}(\text{HPO}_4)_2 \cdot \text{H}_2\text{O}$  <sup>11</sup> and stercorite  $\text{Na}(\text{NH}_4)\text{HPO}_4 \cdot 4\text{H}_2\text{O}$ . These minerals occur as  
31    stalactites and as crusts on the walls and floors of the Caves. Other minerals found in the  
32    Moorba Cave include tanarakite, ardealite, hydroxylapatite, calcite and gypsum. These  
33    minerals are formed through the chemical reactions of calcite with bat guano. These Moorba  
34    Caves have been in existence for eons of time and have been dated as more than 350 million  
35    years old.

36    The minerals monetite  $\text{CaHPO}_4$  and brushite  $\text{CaHPO}_4 \cdot 4\text{H}_2\text{O}$  have been widely studied <sup>12-15</sup>. In  
37    terms of spectroscopy, the minerals are important because of their existence in kidney stones  
38    and other biological materials <sup>3,4,16,17</sup>. S.D. Ross in Farmer’s treatise (page 393) <sup>18</sup> reported  
39    the infrared spectrum of brushite. Data for two mineral samples were provided. However, the  
40    results of the two analyses differ. The  $v_1$  symmetric stretching mode was given as occurring  
41    at  $1005 \text{ cm}^{-1}$ ,  $v_2$  bending mode at 400 and  $418 \text{ cm}^{-1}$ ,  $v_3$  antisymmetric stretching mode at 1075  
42    and  $1135 \text{ cm}^{-1}$ , and the  $v_2$  bending mode at  $577 \text{ cm}^{-1}$ . Multiple OH stretching vibrations were  
43    observed. Other bands associated with the  $\text{HPO}_4$  units were found at 750, 875 and  $1217 \text{ cm}^{-1}$ .

44

45    Raman spectroscopy has proven most useful for the study of mineral structure. The detailed  
46    comparative Raman spectra of the Cave minerals have not been published. In order to test  
47    the brushite from Caves, brushite was synthesised in the laboratory to find how easy the  
48    mineral is to form. The idea is to mimic the chemical reactions in the Caves. The objective of  
49    this research is to report the Raman spectra of brushite and to relate the spectra to the mineral  
50    structure.

51    **Experimental**

52    **Synthesis of brushite**

53    The chemicals were purchased as follows: sodium phosphate dibasic from Sigma-Aldrich  
54    and calcium chloride from Ajax Chemicals. A calcium chloride solution was prepared by  
55    dissolving calcium chloride (25 g) in 100ml water, while a solution of sodium phosphate was  
56    made by dissolving sodium phosphate dibasic (32 g) in 600ml of water. To a 1 L beaker,  
57    100ml of deionised water was added (with agitation), along with the simultaneous addition of  
58    calcium chloride (20 mL) and sodium phosphate (120 mL) solutions. The pH of the resultant  
59    solution was maintained between 4 and 5, using a sodium di-hydrogen phosphate solution to  
60    reduce the pH or a sodium carbonate solution to increase the pH. Two appropriate pumps  
61    were used to control the flow rates of addition to ensure both  $\text{CaCl}_2$  and  $\text{Na}_2\text{HPO}_4$  solutions  
62    completed at the same time. The temperature of precipitation was 25 °C. The solids were  
63    separated from the liquid by centrifugation, washed with deionised water, and dried overnight  
64    at 105 °C in an oven.

65

66    **Natural Mineral**

67    The mineral brushite was supplied by the Australian Museum (mineral sample number  
68    D43843) and originated from Moorba Cave, Jurien Bay, Dandaragan Shire, Western  
69    Australia, Australia. Details of the mineral have been published (page 83)<sup>19</sup>.

70

71    **X-ray diffraction**

72    The ‘Cave’ mineral brushite was placed upon an ultra thin film of paraffin wax (Vaseline). In  
73    this way a minimal amount of the quite precious ‘Cave’ mineral brushite is used. X-ray  
74    diffraction patterns were collected using a Philips X'pert wide angle X-ray diffractometer,  
75    operating in step scan mode, with  $\text{Cu K}\alpha$  radiation ( $1.54052 \text{ \AA}$ ). The Philips PANalytical  
76    X'pert PRO diffractometer was operating at 40 kV and 40 mA with  $0.25^\circ$  divergence slit,  
77     $0.25^\circ$  anti-scatter between  $5$  and  $15^\circ$  ( $2\theta$ ) at a step size of  $0.0167^\circ$ . For XRD at low angle  
78    section, it was between  $1.5$  and  $8^\circ$  ( $2\theta$ ) at a step size of  $0.0167^\circ$  with variable divergence slit  
79    and  $0.125^\circ$  anti-scatter.

80

81 **Raman spectroscopy**

82 Crystals of brushite were placed on a polished metal surface on the stage of an Olympus  
83 BHSM microscope, which is equipped with 10x, 20x, and 50x objectives. The microscope is  
84 part of a Renishaw 1000 Raman microscope system, which also includes a monochromator, a  
85 filter system and a CCD detector (1024 pixels). The Raman spectra were excited by a  
86 Spectra-Physics model 127 He-Ne laser producing highly polarised light at 633 nm and  
87 collected at a nominal resolution of  $2\text{ cm}^{-1}$  and a precision of  $\pm 1\text{ cm}^{-1}$  in the range between  
88 100 and  $4000\text{ cm}^{-1}$ . Repeated acquisition on the crystals using the highest magnification (50x)  
89 was accumulated to improve the signal to noise ratio in the spectra. Spectra were calibrated  
90 using the  $520.5\text{ cm}^{-1}$  line of a silicon wafer.

91 **Infrared spectroscopy**

92 Infrared spectra were obtained using a Nicolet Nexus 870 FTIR spectrometer with a smart  
93 endurance single bounce diamond ATR cell. Spectra over the  $4000\text{--}525\text{ cm}^{-1}$  range were  
94 obtained by the co-addition of 128 scans with a resolution of  $4\text{ cm}^{-1}$  and a mirror velocity of  
95  $0.6329\text{ cm/s}$ . Spectra were co-added to improve the signal to noise ratio. The infrared spectra  
96 are provided in the supplementary information.

97 Band component analysis was undertaken using the Jandel ‘Peakfit’ (Erkrath,  
98 Germany) software package which enabled the type of fitting function to be selected and  
99 allowed specific parameters to be fixed or varied accordingly. Band fitting was done using a  
100 Lorentz-Gauss cross-product function with the minimum number of component bands used  
101 for the fitting process. The Lorentz-Gauss ratio was maintained at values greater than 0.7 and  
102 fitting was undertaken until reproducible results were obtained with squared correlations ( $r^2$ )  
103 greater than 0.995. Band fitting of the spectra is quite reliable providing there is some band  
104 separation or changes in the spectral profile.

105 **Results and discussion**

106

107 **X-ray diffraction**

108 The XRD patterns of the synthesised brushite and the Cave mineral brushite are displayed in  
109 the supplementary Information in Figs. S1a and S1b respectively. The XRD pattern of the  
110 brushite matches that of the reference pattern exactly. The XRD of the Cave mineral brushite  
111 clearly proves that the collected mineral sample was indeed brushite. Traces of calcite and  
112 quartz may also be observed but are minor components. The peak at around 45 degrees two  
113 theta is due to the presence of paraffin wax.

114

## 115 **Raman Spectroscopy**

116 The Raman spectra of synthesised brushite and the Cave mineral in the 650 to 1200 cm<sup>-1</sup>  
117 region are shown in Fig. 1a and in Fig. 1b respectively. The infrared spectrum in the 500 to  
118 1250 cm<sup>-1</sup> region of the synthesised brushite and the natural brushite are displayed in Figs.  
119 S2a and S2b. For the synthetic brushite four Raman bands are observed at 987, 1000, 1063  
120 and 1085 cm<sup>-1</sup>, While for the Cave mineral, three bands are observed at 985, 1000 and 1055  
121 cm<sup>-1</sup>. It is noted that there are some differences in the position f the bands between the  
122 brushite analogue and the Cave mineral. Perhaps this is not unexpected as the Cave brushite  
123 may have some minor partial substitution.

124 These bands are assigned as follows: 987 cm<sup>-1</sup> v<sub>1</sub> PO<sub>4</sub><sup>3-</sup>, 1000 cm<sup>-1</sup> v<sub>1</sub> HPO<sub>4</sub><sup>2-</sup>, and 1063 and  
125 1085 cm<sup>-1</sup>v<sub>3</sub> PO<sub>4</sub><sup>3-</sup> stretching modes. In the infrared spectrum (Fig. S2a.) of the synthesised  
126 brushite, these bands are observed at 987, 1004 and 1061 cm<sup>-1</sup>. The first two bands display  
127 considerable band overlap. In addition, infrared bands are observed at 1118 and 1137 cm<sup>-1</sup>  
128 and are assigned to the v<sub>3</sub> HPO<sub>4</sub><sup>2-</sup> antisymmetric stretching modes. For the Cave mineral,  
129 infrared bands are observed in similar positions. An intense band is observed at 985 cm<sup>-1</sup>  
130 with a shoulder at 1002 cm<sup>-1</sup>. Other infrared bands are found at 1056, 1114, 1131 and 1151  
131 cm<sup>-1</sup>.

132

133 An infrared band for synthetic brushite is observed at 1207 cm<sup>-1</sup>. For the natural brushite, two  
134 bands at 1200 and 1219 cm<sup>-1</sup> are observed. These bands are attributed to the OH in-plain  
135 deformation modes of HPO<sub>4</sub><sup>2-</sup> units. Farmer <sup>18</sup> reported infrared bands at 1200 and 1215 cm<sup>-1</sup>  
136 for brushite and allocated these bands to δ in-plain OH deformations. Indeed the infrared

137 spectrum of brushite based upon the work of Petrov<sup>20-22</sup> is identical to the infrared spectrum  
138 of synthetic brushite reported in this work.

139

140 The Raman spectrum of synthetic brushite in the 300 to 650 cm<sup>-1</sup> region is displayed in Fig.  
141 2a. The Raman spectrum of Cave brushite in the low wavenumber region is displayed in  
142 Fig. 2b. For the synthetic brushite two bands are found at 577 and 587 cm<sup>-1</sup>. A low intensity  
143 band at 576 cm<sup>-1</sup> is found for the Cave brushite. The Raman bands at 577 and 587 cm<sup>-1</sup> are  
144 assigned to the v<sub>4</sub> PO<sub>4</sub><sup>3-</sup> bending mode. It should be kept in mind that the natural brushite  
145 occurs as a powdered deposit on clacite surfaces. Obviously there will be intensity  
146 differences when compared with a highly crystalline synthetic analogue. Intensity  
147 differences can arise from the crystallite orientation and polarization. This vibrational mode  
148 (v<sub>4</sub> PO<sub>4</sub><sup>3-</sup> bending mode) is observed in the infrared spectrum at 579 cm<sup>-1</sup> (Fig. S2a). The  
149 band is found at 577 cm<sup>-1</sup> for the Cave brushite (Fig. 2b).

150 The band occurs in different positions for the hydrogen phosphate anion. This v<sub>4</sub> band for the  
151 HPO<sub>4</sub><sup>2-</sup> anion for the synthetic brushite occurs at 524 and 541 cm<sup>-1</sup>. The band is observed at  
152 519 cm<sup>-1</sup> for the Cave brushite. These bands are not observed in the infrared spectrum as the  
153 cell absorbs all the radiation below 550 cm<sup>-1</sup>. Ardealite Ca<sub>2</sub>(HPO<sub>4</sub>)(SO<sub>4</sub>)·4H<sub>2</sub>O is a mineral  
154 which also contains the hydrogen phosphate anion. Intense Raman bands are found at 505  
155 and 528 cm<sup>-1</sup> for ardealite and are assigned to the v<sub>4</sub>(HPO<sub>4</sub>)<sup>2-</sup> bending modes. It is probable  
156 that the bending modes of OPO and HOPO bending modes occur at the same energy, thus  
157 two distinct bands are not observed. The mineral newberyite Mg(PO<sub>3</sub>OH)·3H<sub>2</sub>O also contains  
158 a hydrogen phosphate anion. The Raman spectrum of this mineral has been reported<sup>23</sup>. An  
159 intense band was observed for this mineral at 498 cm<sup>-1</sup>. Rajendran and Keefe<sup>24</sup> reported  
160 Raman bands at 521 and 586 cm<sup>-1</sup> and assigned these bands to (H-O)P=O absorption bands.  
161 This assignment is in contrast to the assignment of bands by Ross<sup>18</sup>.

162

163 For the synthetic brushite, Raman bands are found at 379 and 411 cm<sup>-1</sup> and are assigned to v<sub>2</sub>  
164 PO<sub>4</sub><sup>3-</sup> bending modes. For the Cave mineral a Raman band is found at 411 cm<sup>-1</sup>. Farmer<sup>18</sup>  
165 based upon the work of Petrov *et al.* reported these bands at 400 and 418 cm<sup>-1</sup> which is in  
166 agreement with the assignations of this work. It is interesting that these vibrations for the

167 aqueous  $\text{HPO}_4^{2-}$  anion occur at much lower wavenumbers (278 and 318  $\text{cm}^{-1}$ ). In the infrared  
168 spectrum, bands are observed at 795  $\text{cm}^{-1}$  with shoulder bands at 734 and 860  $\text{cm}^{-1}$ . These  
169 bands are assigned to the out-of-plane vibrations of POH units. Farmer<sup>18</sup> tabled this band at  
170 750  $\text{cm}^{-1}$ .

171 The Raman spectrum of the synthesised brushite analogue and the natural Cave mineral in the  
172 far low wavenumber region are displayed in Figs. 3a and 3b respectively. The synthetic  
173 brushite in this spectral region is characterised by an intense band at 205  $\text{cm}^{-1}$ . The band is  
174 assigned to a librational mode and shows sensitivity to disorder. The band is broad and of  
175 low intensity for the natural brushite. This disorder can arise through a partial substitution of  
176 calcium ions by other ions for example  $\text{Mg}^{2+}$  and  $\text{H}^+$ .

177

178 The bands at 879  $\text{cm}^{-1}$  for synthetic brushite (Figure 1a) and at 872  $\text{cm}^{-1}$  (Figure 2b) for the  
179 Cave brushite are assigned to the symmetric stretching vibrations of the POH units. Ross in  
180 Farmer<sup>18</sup> reported this band at 875  $\text{cm}^{-1}$ . A Raman band is found at 862  $\text{cm}^{-1}$  for ardealite.  
181 The two infrared bands at 651 and 672  $\text{cm}^{-1}$  for synthetic brushite may be due to water  
182 librational modes. The bands are observed at 649 and 669  $\text{cm}^{-1}$  for Cave brushite.

183 The position of this band is in harmony with the band position of the aqueous hydrogen  
184 phosphate anion at 891  $\text{cm}^{-1}$ <sup>25</sup>. This band is assigned to the  $\nu_1 \text{HPO}_4^{2-}$  symmetric stretching  
185 mode. The band is due to the presence of hydrogen phosphate units in the ardealite structure.  
186 A Raman band was observed in the spectrum of newberyite  $\text{Mg}(\text{PO}_3\text{OH})\cdot 3\text{H}_2\text{O}$  at 887  $\text{cm}^{-1}$   
187 and is attributed to  $\text{HPO}_4^{2-}$  symmetric stretching mode<sup>23</sup>. Such bands are normally intense in  
188 the infrared spectrum but of low intensity in the Raman spectrum. Rajendran and Keefe<sup>24</sup>  
189 studied the growth and characterisation of calcium hydrogen phosphate dihydrate and  
190 reported the FTIR and Raman spectra. These researchers observed a band at 875  $\text{cm}^{-1}$  and  
191 assigned this band to the  $\text{HPO}_4^{2-}$  POP antisymmetric stretching mode. However, this  
192 assignment differs from the interpretation reported in this work.

193

194 The Raman spectrum of synthetic brushite in the 3000 to 3800  $\text{cm}^{-1}$  region and the Raman  
195 spectrum of Cave brushite are shown in Figs. 4a and 4b respectively. In the Raman spectrum,  
196 four bands are observed at 3166, 3265, 3470 and 3540  $\text{cm}^{-1}$ . The bands are assigned to the

197 symmetric stretching modes of water. Two Raman bands are observed for Cave brushite at  
198 3472 and 3533 cm<sup>-1</sup>. Other bands may be present but the signal to noise ratio is low and  
199 consequently other water bands could not be identified. The infrared spectrum of synthetic  
200 brushite in the 2500 to 4000 cm<sup>-1</sup> region and the infrared spectrum of Cave brushite in the  
201 3000 to 3700 cm<sup>-1</sup> region are shown in Figs. S3a and S3b respectively. In the infrared  
202 spectrum of synthetic brushite, bands are found at 3157, 3275, 3477 and 3539 cm<sup>-1</sup>.  
203 Additional infrared bands for synthetic brushite are observed at 2972, 3157, 3275 and 3384  
204 cm<sup>-1</sup> and are also assigned to water stretching bands. For the Cave brushite, infrared bands  
205 are observed at 3154, 3269, 3475 and 3537 cm<sup>-1</sup>. The infrared spectra are in harmony with  
206 the Raman data which clearly shows the existence of non-equivalent water molecules in the  
207 brushite structure.

208

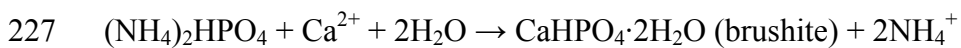
209 Jones and Smith <sup>26</sup> reported the OH wavenumbers for the related mineral monetite. Berry and  
210 Baddiel <sup>27,28</sup> interpreted the infrared spectrum of brushite in terms of the hydrogen phosphate  
211 anion and proposed that the infrared spectrum was based upon the occupation of C<sub>2</sub> sites by  
212 HPO<sub>4</sub><sup>2-</sup> ions. Ross in Farmer <sup>18</sup> stated that the two possible space groups are C<sub>s</sub><sup>4</sup> and C<sub>2h</sub><sup>6</sup>. The  
213 first space group is favoured and the centrosymmetric space group requires all eight water  
214 molecules in brushite to be equivalent. The infrared spectrum of brushite clearly shows  
215 multiple water bands involving different hydrogen bond strengths, thus indicating the water  
216 molecules are not all equivalent in the brushite structure. Crystallographic studies show that  
217 there are five crystallographic independent hydrogen atoms in the crystal structure of brushite  
218 with z=4 in the non-centrosymmetric monoclinic space group Ia <sup>29</sup>. In the structure, two  
219 water molecules coordinate differently with different hydrogen bond strengths as indicated by  
220 the hydrogen bond distances <sup>29</sup>.

221

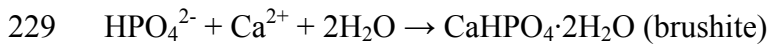
## 222 **Mechanism of formation of brushite**

223

224 Brushite is formed on calcite surfaces in the Moorba Caves. The source of the phosphate ion  
225 is bat guano and is probably present as an ammonium hydrogen phosphate or related  
226 chemical. The following reaction is proposed:



228 Alternatively the equation may be written as



230 The calcium ions originate from the dissolution of calcite. Carbonate ions function as an  
231 inhibitor of the calcium phosphates. This fact suggests that brushite is formed in solution and  
232 is translocated through the Cave system and then precipitates from solution, as is shown in  
233 the above equation.

234 For the synthesised brushite the following reaction is proposed:



236

237 The mineral brushite is formed in renal canals and urinary calculus<sup>6,7,27,30,31</sup>. The proposed  
238 chemical reaction above is a mechanism for the formation of brushite in these renal and  
239 urinary calculus<sup>32-34</sup>. It is probable that the concentration of calcium ions effects the  
240 formation of brushite. High concentrations of  $\text{Ca}^{2+}$  favours brushite formation, as is found in  
241 Caves such as in the Moorba and Jenolan Caves.

242

### 243 **Conclusions**

244 Brushite was synthesised in order to match the chemical reaction that occurs in Cave systems  
245 through the reaction of bat guano with calcite. Brushite is a mineral of significance because  
246 of its formation in the urinary tract. No doubt this type of reaction occurs in the urinary tract.  
247 The XRD patterns of both the synthesised brushite and the Cave mineral brushite show  
248 identical patterns to the standard brushite XRD pattern. The Cave mineral brushite contains  
249 minerals other than brushite whereas the synthesised brushite is pure. A mechanism of  
250 formation of brushite in Caves is proposed. This mechanism is probably the same type of  
251 chemical reaction that occurs in renal canals.

252 Even though the Raman spectrum of the Cave mineral brushite suffers from a lack of signal  
253 to noise, the Raman spectrum of the Cave mineral brushite closely resembles that of the  
254 synthesised mineral.

255

256 **Acknowledgments**

257 The financial and infra-structure support of the Queensland University of Technology,  
258 Chemistry discipline is gratefully acknowledged. The Australian Research Council (ARC) is  
259 thanked for funding the instrumentation.

260

## 261 REFERENCES

- 262 (1) Hill CA *Cave Minerals*, 1976.  
263 (2) White WB *Sci. Speleol.* **1976**, 267.  
264 (3) Casciani F, Condrate RA *Spectrosc. Lett.* **1979**, 12, 699.  
265 (4) Kodati VR, Tomasi GE, Turumin YL, Tu AT *Appl. Spectrosc.* **1991**, 45, 581.  
266 (5) Kumar M, Xie J, Chittur K, Riley C *Biomaterials* **1999**, 20, 1389.  
267 (6) Santos M, Garcia-Ramos JV, Bellanato J, Carmona P, Cifuentes-Delatte L  
268 *Fortschr. Urol. Nephrol.* **1984**, 22, 405.  
269 (7) Sudlow K, Woolf A *Clin. Chim. Acta* **1991**, 203, 387.  
270 (8) Dumitras D-G, Marincea S, Fransolet A-M *Neues Jahrb. Mineral., Abh.* **2004**,  
271 180, 45.  
272 (9) Marincea S, Dumitras D-G, Diaconu G, Bilal E *Neues Jahrb. Mineral.,*  
273 *Monatsh.* **2004**, 464.  
274 (10) Bridge PJ *Mineral. Mag.* **1977**, 41, 33.  
275 (11) Bridge PJ, Clark RM *Mineral. Mag.* **1983**, 47, 80.  
276 (12) Ronson TK, McQuillan AJ *Langmuir* **2002**, 18, 5019.  
277 (13) Soprajanov B, Jovanovski G, Kuzmanovski I, Stefov V *Spectrosc. Lett.* **1998**,  
278 31, 1191.  
279 (14) Soprajanov B, Kuzmanovski I, Stefov V, Jovanovski G *Spectrosc. Lett.* **1999**,  
280 32, 703.  
281 (15) Tortet L, Gavarri JR, Nihoul G, Dianoux AJ *J. Solid State Chem.* **1997**, 132, 6.  
282 (16) Benramdane L, Bouatia M, Idrissi MOB, Draoui M *Spectrosc. Lett.* **2008**, 41,  
283 72.  
284 (17) Essaddek A, Elgadi M, Mejdoubi E, Elansari LL, Moradi K, Karroua M *J.  
285 Phys. IV* **2005**, 123, 233.  
286 (18) Farmer VC *Mineralogical Society Monograph 4: The Infrared Spectra of  
287 Minerals*, 1974.  
288 (19) Anthony JW, Bideaux RA, Bladh KW, Nichols MC *Handbook of Mineralogy  
289 Vol. IV. Arsenates, phosphates, vanadates - Mineral Data Publishing, Tucson, Arizona;*  
290 *Mineral data Publishing: Tucson, Arizona, 2000; Vol. IV.*  
291 (20) Mitchell PCH, Parker SF, Simkiss K, Simmons J, Taylor MG *J. Inorg.  
292 Biochem.* **1996**, 62, 183.  
293 (21) Petrov I, Soprajanov B, Fuson N *Z. Anorg. Allg. Chem.* **1968**, 358, 178.  
294 (22) Petrov I, Soprajanov B, Fuson N, Lawson JR *Spectrochim. Acta, Part A* **1967**,  
295 23, 2637.  
296 (23) Frost RL, Weier ML, Martens WN, Henry DA, Mills SJ *Spectrochimica Acta,  
297 Part A: Molecular and Biomolecular Spectroscopy* **2005**, 62A, 181.  
298 (24) Rajendran K, Keefe CD *Cryst. Res. technol.* **2010**, 45, 939.  
299 (25) Ross SD *Inorganic infrared and Raman spectra*; McGraw-Hill: Maiden-Head,  
300 UK, 1972.  
301 (26) Jones DW, Smith JAS *Trans. Faraday Soc.* **1960**, 56, 638.  
302 (27) Berry EE *Spectrochim. Acta, Part A* **1968**, 24, 1727.  
303 (28) Berry EE, Baddiel CB *Spectrochim. Acta, Part A* **1967**, 23, 2089.  
304 (29) Curry NA, Jones DW *J. Chem. Soc. A* **1971**, 3725.  
305 (30) Daudon M, Marfisi C, Lacour B, Bader C *Clin. Chem. (Winston-Salem, N. C.)*  
306 **1991**, 37, 83.  
307 (31) Parker SF, Mitchell PCH, Simkiss K, Simmons J, Taylor MG *Biol. Macromol.  
308 Dyn., Proc. Workshop Inelastic Quasielastic Neutron Scattering Biol.* **1997**, 37.

309 (32) Pak CYC *J. Clin. Invest.* **1969**, *48*, 1914.  
310 (33) Pak CYC *J. Cryst. Growth* **1981**, *53*, 202.  
311 (34) Pak CYC, Cox JW, Powell E, Bartter FC *Amer. J. Med.* **1971**, *50*, 67.  
312  
313

314

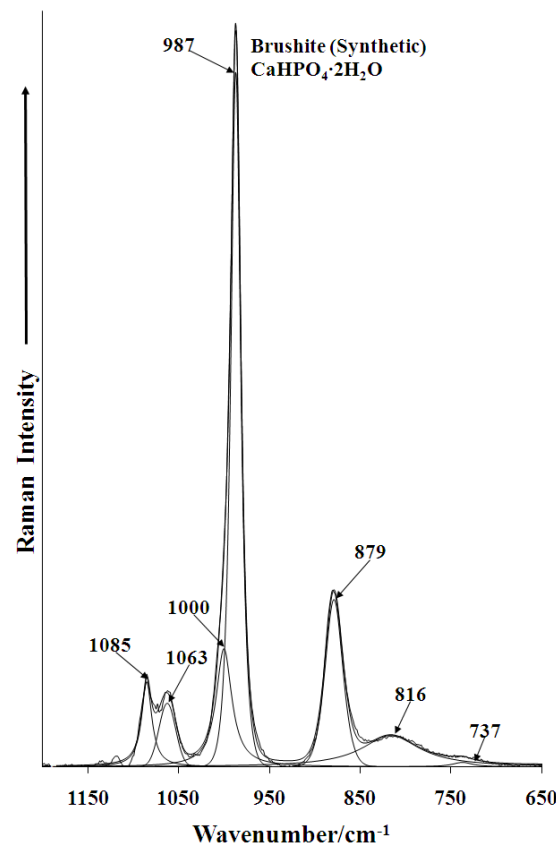
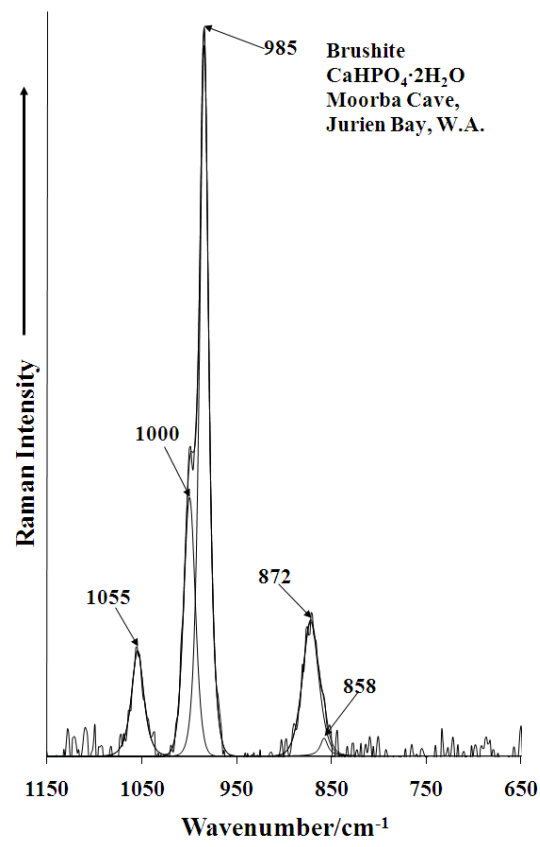
315

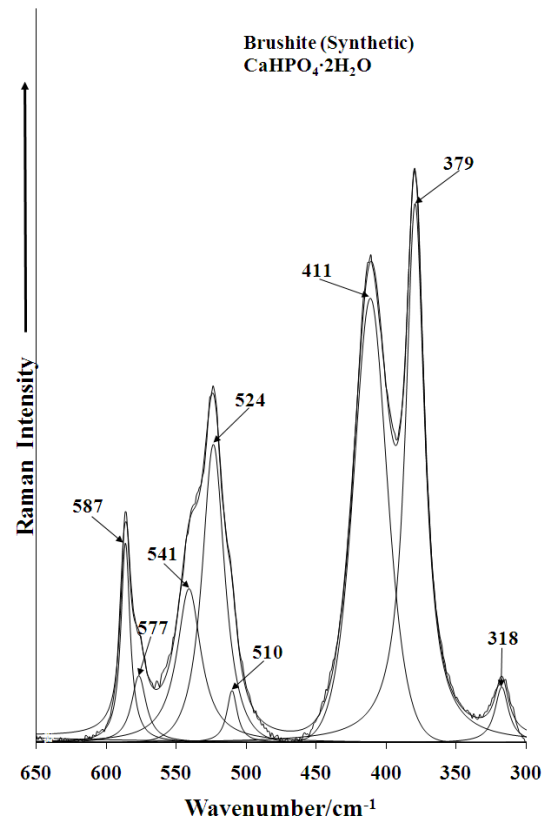
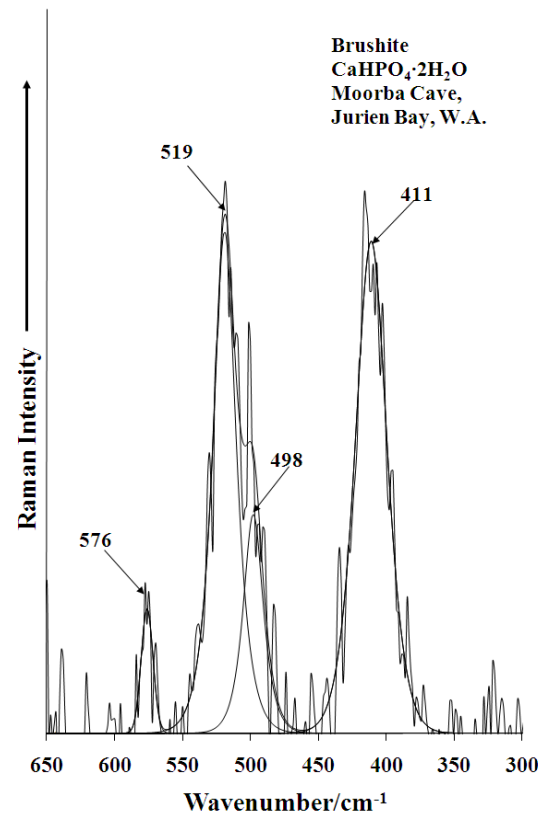
316

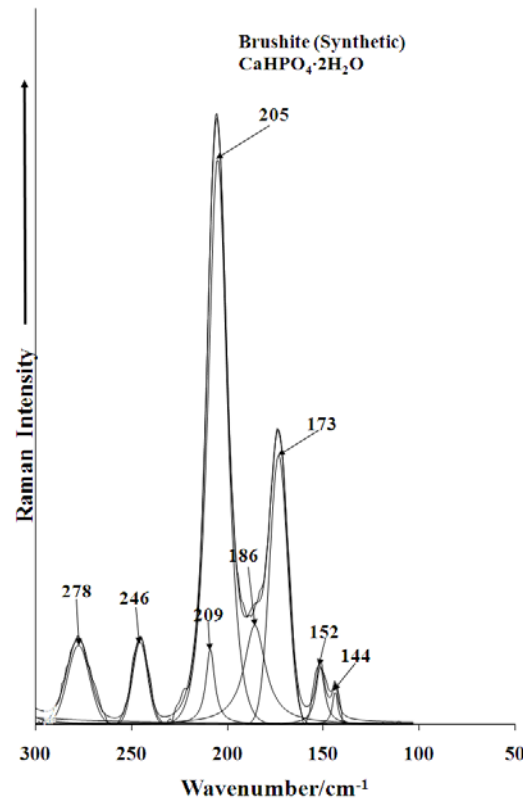
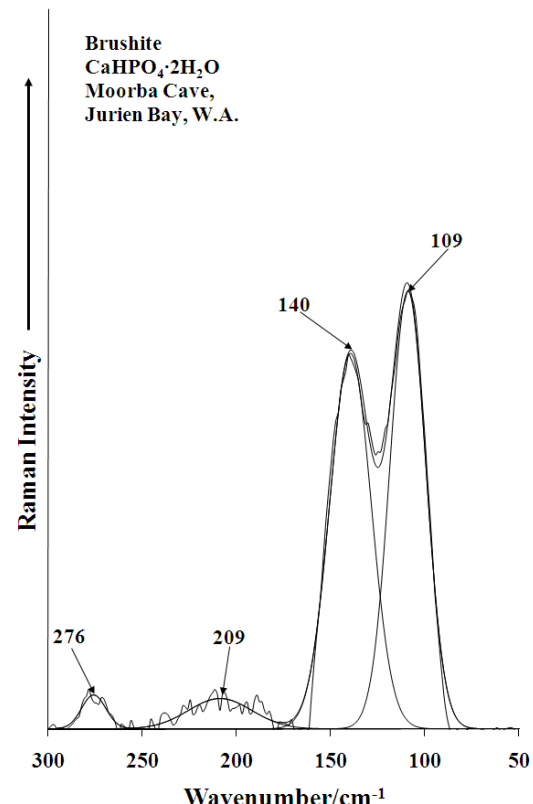
317

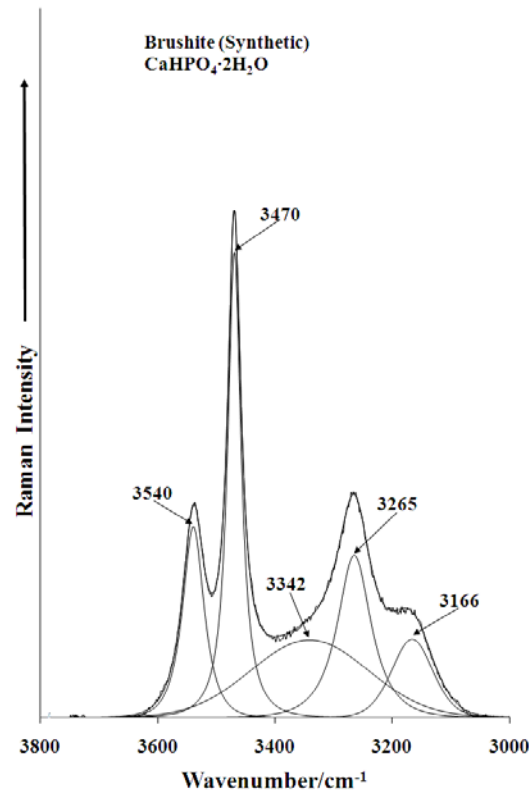
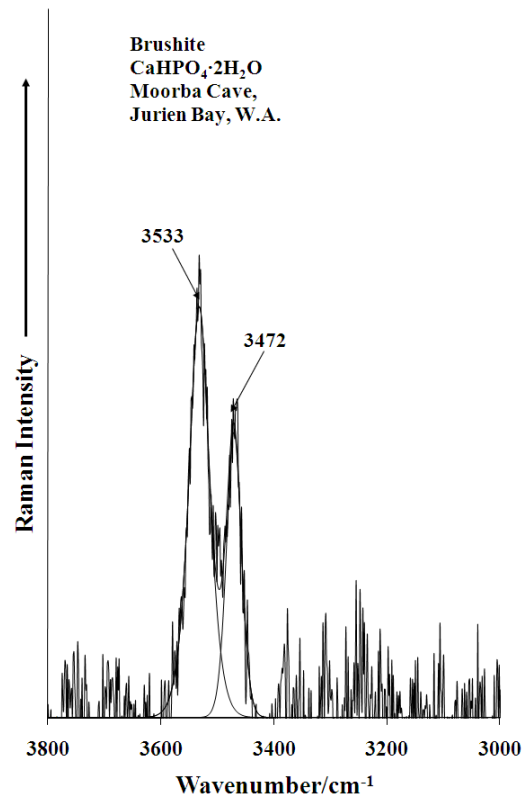
318 **List of Figures**

- 319 **Figure 1a Raman spectra of synthetic brushite from 650 to 1200 cm<sup>-1</sup>.**
- 320 **Figure 1b Raman spectra of the Cave mineral brushite from 650 to 1150 cm<sup>-1</sup>.**
- 321 **Figure 2a Raman spectra of synthetic brushite from 300 to 650 cm<sup>-1</sup>.**
- 322 **Figure 2b Raman spectra of the Cave mineral brushite from 300 to 650 cm<sup>-1</sup>.**
- 323 **Figure 3a Raman spectra of synthetic brushite from 100 to 300 cm<sup>-1</sup>.**
- 324 **Figure 3b Raman spectra of the Cave mineral brushite from 50 to 300 cm<sup>-1</sup>.**
- 325 **Figure 4a Raman spectra of synthetic brushite from 3000 to 3800 cm<sup>-1</sup>.**
- 326 **Figure 4b Raman spectra of the Cave mineral brushite from 3000 to 3800 cm<sup>-1</sup>.**
- 327
- 328
- 329
- 330
- 331
- 332
- 333
- 334
- 335
- 336
- 337

**Figure 1a****Figure 1b**

**Figure 2a****Figure 2b**

**Figure 3a****Figure 3b**

**Figure 4a****Figure 4b**